An Analysis of the Bearing Capacity Ratio of the Cavitation-Prone Gypsum Soil

Sarab Siham Tawfeeq
Department of Civil Engineering, College of Engineering, University of Tikrit, Salah Al-Din, 34001, Iraq.
sarab.najem@tu.edu.iq (corresponding author)

Received: 8 May 2025 | Revised: 24 May 2025 and 7 June 2025 | Accepted: 9 June 2025

 DOI: https://doi.org/10.48084/etasr.12010

ABSTRACT

Gypsum soils, commonly found in semi-arid and arid regions, are susceptible to water exposure, which can lead to cavities that significantly reduce their ability to sustain loads. This research examines the impact of gypsum concentration, dissolution rates, and geometric parameters on the Bearing Capacity Ratio (BCR). Four soils with varying concentrations of gypsum and dissolution rates were investigated for both concentrated and eccentric load conditions using Finite Element Modeling (FEM). The results showed that increasing the L/B ratio (ratio of the horizontal distance (L) between the cavity center and foundation centerline to the foundation width (B)) improved the load distribution, especially for low-solubility soils, and reduced the effect of cavities on the stress distribution. However, soils with more significant dissolution rates, such as soil III (40% dissolution), did not perform well due to severe cavitation. The statistical analysis revealed that the soil type and dissolution levels were the most significant factors controlling BCR. The regression analysis enabled the creation of a predictive formula that incorporates essential factors, such as geometric ratios and gypsum dissolution. Soil I (0% dissolution) always exhibited greater BCR values, while soil III (40% dissolution) exhibited an extreme decline in BCR due to the extensive cavities formed by dissolution mechanisms. The soil without gypsum dissolution showed the highest bearing capacity ratio. Increased dissolution reduced the bearing capacity due to weakening caused by the formation of cavities. Increasing the depth-to-horizontal distance ratios improved the load distribution and bearing capacity, especially in soils with lower dissolution rates. The eccentric forces resulted in disparate strain rates adjacent to the load, thereby decreasing the bearing capacity in cavities nearby. Especially in settings with high gypsum concentrations, the study emphasizes the need to control the dissolution rates of gypsum and optimise geometric ratios in foundation structures. For designers seeking to forecast and mitigate foundation failure in gypsum-rich soils, the study provides valuable insights.

Keywords-gypsum soils; bearing capacity ratio; cavity; dissolution rate; eccentric load

I. INTRODUCTION

Cavities are a factor in the analysis of shallow foundation bearing capacity in geotechnical design. Cavities are often formed by natural geological phenomena like gypsum dissolution or karstification. They may pose serious risks to the stability of structures, such as unexpected settlement, foundation failures, and even the collapse of buildings on gypsum-rich or karstic soils. The design and construction of the foundation are made challenging by the inconsistent distribution of these cavities as it interact with the foundation loads. Therefore, using suitable analytical and numerical techniques to estimate the ultimate bearing capacity of the overlying cavities of foundations is crucial to providing the safety and durability of such structures [1-2].

Many studies have been conducted to understand further the connection between the underlying cavities and the functionality of shallow foundations. The authors in [3], for instance, modelled the impact of irregular voids in karstic soils using the Upper Bound Finite Element Limit Analysis method. They have noticed that the strip foundation bearing capacity may reduce by as much as 40% when cavities form at shallow locations from the ground surface compared to a no-void condition. They employed Plaxis 2D to analyze further the case of the ground cavities in sandy-clay soil that had been exposed to both centred and eccentric loads. According to the findings, eccentric loading significantly reduces bearing capacity; however, this decrease can be mitigated by up to 25% with the use of geogrid reinforcement. Hence, reinforcement offers a way to lessen the instability caused by cavities [4].

Authors in [5] focused on the cavity size and spacing, while applying the Randomised Particle Finite Element Method (RPFEM) to analyze the bearing capacity of shallow foundations over cavities. It was found that as the size of the cavity increases, the bearing capacity decreases by about 30%, which shows that the geometry of the cavity is an important factor in stability analysis. Furthermore, the study demonstrated that ANN techniques can accurately predict the bearing capacity of reinforced soils with an accuracy of more than 95%, which further highlights the capability of machine

learning techniques as powerful tools for geotechnical analysis [6].

Multiple voids beneath the foundation have also been investigated [7]. According to [8], closely spaced cavities, especially those aligned with the directions of stresses, may reduce the bearing capacity by up to 50%. These findings underscore the importance of employing advanced statistical methodologies to assess the impact of cavity distribution on foundation stability. Meanwhile, authors in [9] proposed an integrated mathematical model for the EPR to predict the cavity effects on bearing capacity with an accuracy of up to 97%, indicating the potential of data-driven approaches in geotechnical engineering.

Despite such advances, some issues remain unaddressed. For example, the gradual dissolution of gypsum soils and the absence of well-established mathematical models for the reliable estimation of BCR remain of great concern. Authors in [10] investigated the behavior of strip footings on cohesionless slopes with underlying circular voids under eccentric loads, showing that the voids' proximity to the foundation's edge promotes instability. Similarly, authors in [11-12] studied the undrained bearing capacity of shallow foundations laid above spherical cavities. They found that shallow cavities remarkably decrease the bearing capacity, and the failure mechanisms are related to the depth-to-diameter ratio of the cavities.

Developments in artificial intelligence have enhanced the accuracy of the bearing capacity predictions. Authors in [13] used ANN for predicting soil properties, such as bearing capacity, internal friction angle, cohesion, and plasticity index, in the soils of Baghdad, and their results supported the reliability of ANN models when applied to the geotechnical area. Moreover, authors in [14] investigated the effect of soil cavities on the shallow foundation bearing capacity resting on a reinforced sandy slope. The test results indicated that geotechnical reinforcement, especially with carbon and glass fibers, significantly reduces the instability due to cavities, particularly when the depth of the cavity exceeds twice the width of the foundation.

As urbanization and infrastructure development continue in gypsum-rich areas, understanding the effects of gypsum dissolution on foundation stability is becoming critical for ensuring safe and durable construction. This research attempts to fill the knowledge gap on BCR, which measures the ability of soil to carry a load before failing, and is affected by factors, such as the gypsum content and dissolution rate. This study investigates the relationship between the BCR and key parameters, such as the depth-to-width ratio (H/B), dissolution levels, and horizontal cavity distance from the foundation centre in gypsum rich soils. Given the unique mechanical behavior of gypsum soils, which are susceptible to dissolution in water, this research develops a reliable mathematical model for BCR estimation. The correlations between these variables and their influence on BCR was studied using multiple regression analysis. The study provides an engineering tool for assessing the mechanical behavior of cavernous soils under various loading conditions, enabling better design efficiency and reducing gypsum soil-related hazards.

II. METHODOLOGY

The impact of soil's gypsum content (X%) and dissolving levels (D%) on foundation stability under varied loads has been studied through modeling based on the cavity width beneath the foundation and the amount of soil that may dissolve. For this purpose, the soil was separated into four main categories, as shown in Table I. This study utilized a 1 m × 1 m square base for analysis. Three main types of cavitation places were examined: cavitation directly below the foundation, cavitation with partial displacement, and cavitation far from the foundation centre. The impact of the cavitation at a distance 0.4 m was further tested by varying the vertical depth (H) and the horizontal displacement (L). In addition, the effects of concentrated and eccentric loads on soil performance were assessed.

To investigate the deformations caused by a concentrated load at X = 0 m, two scenarios of eccentric loading were considered. The load was incrementally increased during the analysis until failure occurred at displacements of 0.1 m and 0.2 m from the foundation center. To understand the relationship between all elements influencing the foundation stability, eighty-four simulation scenarios were developed, encompassing various soil types, dissolving ratios, cavitation sites, and different loading conditions. The gypsum content and dissolution rates were chosen based on typical soil conditions in arid regions, especially in areas like Iraq, where gypsum-rich soils are abundant.

TABLE I. SOIL PROPERTIES AND SPECIFICATIONS

Soil type	Gypsum content ω%	Dissolving (D%)	Cohesion C (kPa)	Friction angle (Ø)
Reference soil	60%	0%	25	40
Soil I	60%	0%	25	40
Soil II	40%	20%	15	30
Soil III	20%	40%	10	18

III. NUMERICAL MODELING

FEM was employed in GeoStudio to simulate the deformation behavior of a foundation located over gypsum soil with cavitation. This technique was chosen for its ability to capture the nonlinear soil-foundation interactions, cavitation effects, and minimize the edge effects, all of which are deemed important by previous studies. A three-dimensional numerical model, with dimensions extending three to five times the foundation width (B) [15], was used to eliminate the boundary effect inaccuracies, as illustrated in Figure 1. A square foundation with dimensions (B × B) was modeled on the soil surface, with a cavity positioned at depth H and horizontal offset L, to assess the effect of cavity location on the foundation stability in gypsum soil.

A hybrid mesh comprising 4,243 nodes and 1,356 elements, with combined quadrilateral and triangular components, was employed to strike a balance between numerical accuracy and computational performance, as proposed by the sensitivity analysis in [16]. Figure 2 depicts the meshing pattern. Quadrilateral elements were assigned to high-stress zones (foundation edges and cavity regions) for improved stress

resolution. In contrast, triangular elements were employed in low-stress areas to ensure computational stability. Fixed boundary constraints were imposed on the lateral and bottom edges to avoid artificial displacements and ensure that the model appropriately reflects the soil behavior beneath the foundation. The soil-foundation contact was assigned to an interface strength reduction factor (R = 1.0), representing the high adhesion characteristic of gypsum soil, which reduces separation under loading circumstances [15, 17].

Instead of traditional stress-strain methods, a load-deformation analysis was employed, which enables a more precise evaluation of the settlement behavior under applied loads. This displacement technique provided important information about cavity-induced deformations and gypsum soil stability.

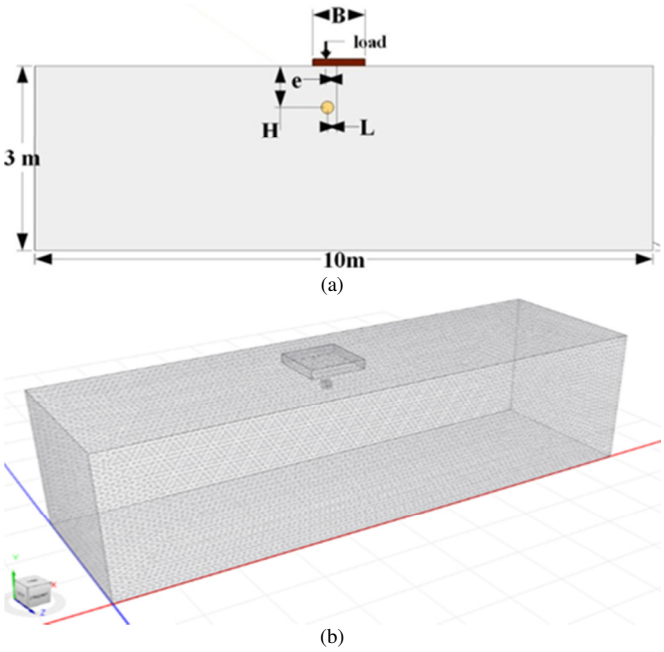

Fig. 1. (a) FEM model setup, (b) mesh configuration.

The Deviatoric Strain Distribution map, shown in Figure 2, depicts the shearing of soil deformation due to different loading conditions. The color gradient represents the strain intensity: red for higher strain and blue for lower strain. This map identifies the stress concentration zones, especially around cavities, where soil failure or excessive settlement is most likely to occur. The high-strain areas predefine the failure zone, whereas the low-strain areas are stable.

The influence of the geometric ratio H/B and L/B on the BCR of soils with a constant 60% gypsum content with different degrees of dissolution were examined. The results show that out of all samples, soil I, which had no disintegration (0%), behaved the best. The lack of the dissolving effect allowed for the stable mechanical characteristics of the soil, strengthening its internal structure and ability to withstand stress. BCR was enhanced significantly by raising H/B since the cavity's direct impact on the foundation decreased as its depth increased. Also, improving the stress distribution by an increase in L/B, improved efficiency, as displayed in Figures 3-5.

Compared to soil I, soil II, which had 20% solubility, performed worse. The soil's internal framework became relatively weak due to the mild voids created by dissolution. However, while the increase in the depth and horizontal distance reduced the influence of cavities on stress distribution and foundation stability, the geometric ratios H/B and L/B continued to help improve BCR. On the other hand, among the three samples, soil III had the lowest BCR, with 40% dissolution. Also, soil's stability to sustain high pressures was significantly reduced due to the big voids created by the high solubility. Even though raising H/B and L/B helped increase BCR, solubility significantly impacted the soil's overall reaction to improving the geometric ratios. These findings demonstrate that the gypsum dissolution is the key element controlling the soil stability. The soils containing insoluble gypsum had the highest BCR and showed higher resistance to deformation. However, higher solubility degrades the soil's mechanical characteristics, diminishing its ability to distribute loads and reducing its bearing capacity. This research highlights the importance of managing the solubility rates and mitigating their impact on soil stability to enhance structural efficiency in areas with high gypsum content.

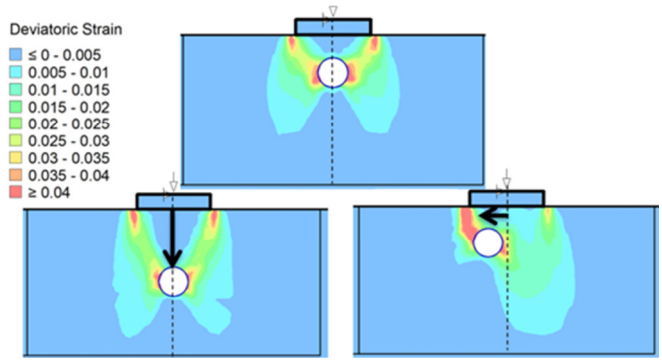

Fig. 2. Deviatoric strain distribution.

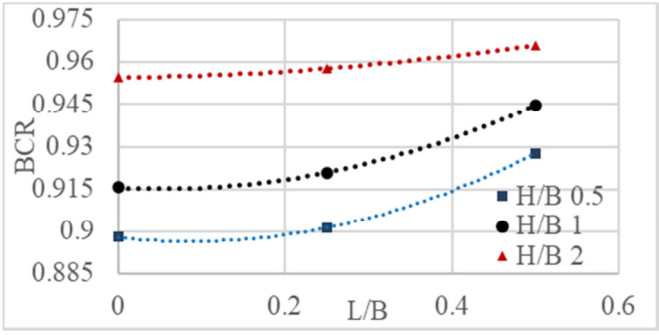

Fig. 3. BCR for soil I is under central load.

The impact of the H/B ratio on BCR at L/B = 0 with concentrated load for the soil types I, II, and III can be seen in Figure 6. The influence of direct cavitation on the stress

distribution reduces with increasing H/B, with deeper cavitation decreasing stresses from the load. Since soil I had no dissolution (0%), greater depths helped maintain relatively stable BCR levels. The effect of depth was more pronounced in reducing stresses in soil II, which had 20% dissolution, but it could not prevent the small performance drop due to cavitation. Soil III (40% dissolution) was the least responsive to the effect of depth, with structural weakening due to significant dissolution remaining the primary factor in reducing BCR. Overall, the findings suggest that increasing the depth does not appear to improve the performance, particularly at higher dissolution ratios.

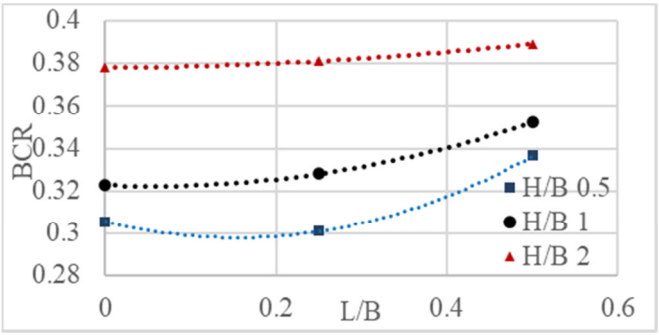

Fig. 4. BCR for soil II is under central load.

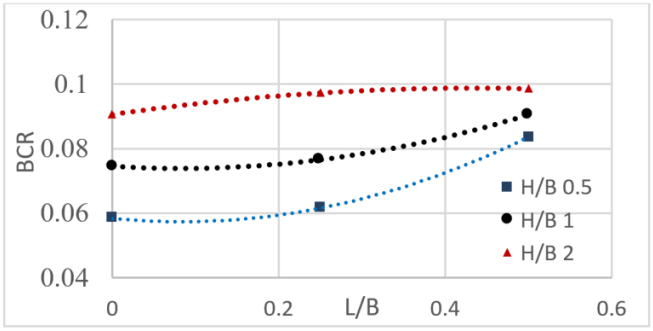

Fig. 5. BCR for soil III is under central load.

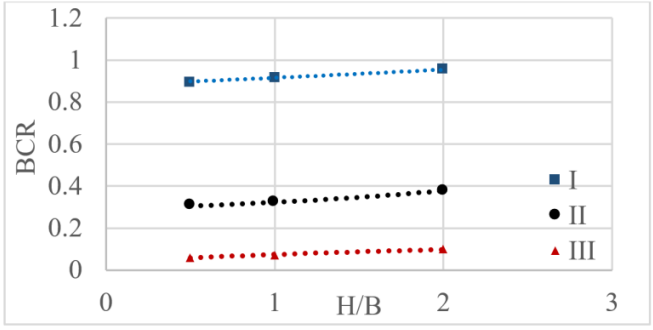

Fig. 6. BCR for all soil types is under central load.

IV. EFFECT OF LOAD ECCENTRICITY

Figures 7-9 portray the deformed shapes of the deviatoric strain distribution in soil II at different eccentricities at e = 0 m, 0.1 m, and 0.2 m for which H/B = 1 and L/B = 0. With the increase in eccentricity, the strain distribution in the soil became highly asymmetric, showing the concentration of strains near the point of load application. The central load in Figure 7 gives a symmetric distribution of the strains, mainly beneath the cavity, while the eccentric loads in Figures 8 and 9 dislocate the strain to the side of the cavity that faces the applied load.

The influence of increased loads on BCR and the cavity's position relative to the foundation center was examined, as shown in Figures 10–12. It is observed that BCR is highly sensitive to the cavity location. When the cavity is located close to the foundation's centre, for L/B = 0, the stress concentrations are directly above the cavity, and the load-carrying capacity of the soil decreases abruptly. For L/B = 0.25, the increase in the horizontal distance of the cavity leads to a gradual improvement in BCR because the influence of the cavity on the stress distribution beneath the foundation diminishes, which results in increasing the stability of the soil.

BCR was influenced the most by the cavity position in soil I, which had no dissolution. It is observed that the BCR shows significant improvement for this soil at L/B = 0.5, indicating mechanical stability to withstand stresses in the presence of cavities. In soil II, which had 20% gypsum dissolution, a sharp decrease in BCR was observed when the cavity was located directly beneath the foundation (L/B = 0). This reduction is primarily due to the voids formed by the dissolution process, which weakened the soil structure, however, BCR improved as L/B was increased. With shifting horizontal distance, the cavity's effect on the stress delivery diminished. However, the location of the cavities had the most significant impact on soil III, which had 40% dissolution. Its BCR decreased significantly for all L/B values, with little change at L/B 0.5. This behavior shows that large-scale voids are created by high its dissolution, which affects the soil's ability to handle loads.

These results indicate the crucial role cavity location plays in determining soil behavior under loading conditions. Concentrations of stress and a rapid decrease in bearing capacity are caused by a cavity close to the center of the foundation, L/B = 0. The ability of the soil has been enhanced by a cavity located further away, L/B = 0.5, which offers a more even distribution of stress. These results further highlight the importance of considering cavity location and its impact on stability when designing a foundation..

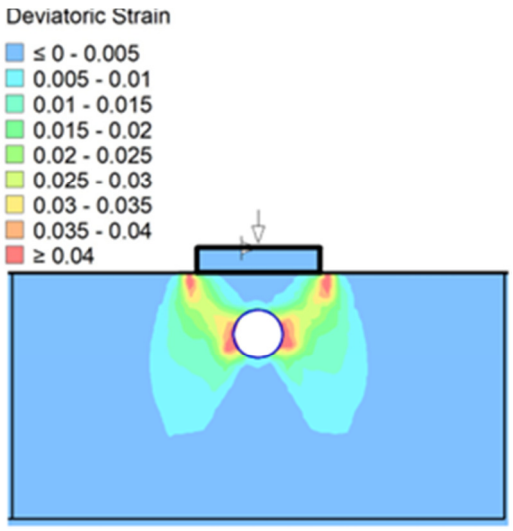

Fig. 7. Deviatoric strain for soil II, with e =0, L/B = 0, and H/B = 1.

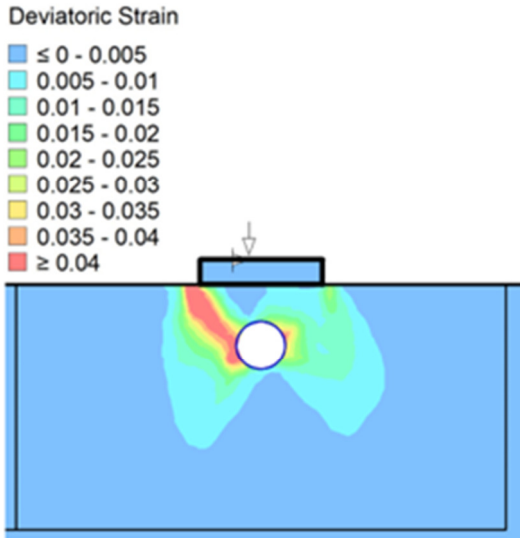

Fig. 8. Deviatoric strain for soil II, with e =0.1 m, L/B = 0, and H/B = 1.

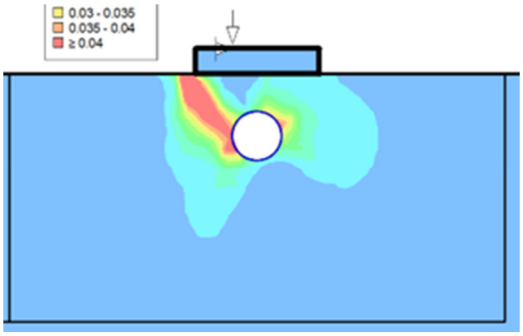

Fig. 9. Deviatoric strain for soil II, with e = 0.2 m, L/B =0, and H/B = 1.

V. ESTIMATION OF BEARING CAPACITY RATIO

Figure 13 presents a statistical survey of the BCR distribution, revealing an asymmetric pattern with a tail extending toward higher values and a concentration of lower values. The low values can be attributed to cavities in the gypsum soil, which are generated by the rapid dissolution of gypsum. These cavities reduce the bulk density of the soil and weaken its internal structure, which leads to a reduction in soil's carrying capacity. On the other hand, the tail that extends to high values represents the outcomes of tests conducted on gypsum soil that dissolves at a slower rate. This improves the soil's bearing capacity by reducing the impacts of cavitation and dissolution. This disparity underscores the significance of reduced dissolution rates in enhancing the properties of gypsum soils and ensuring their stability under loads while also highlighting the substantial impact of the dissolution rate on the geotechnical behavior of soils.

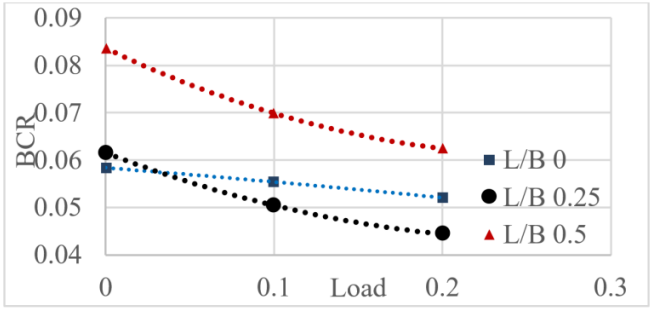

Fig. 10. BCR for soil III at H/B = 0.5.

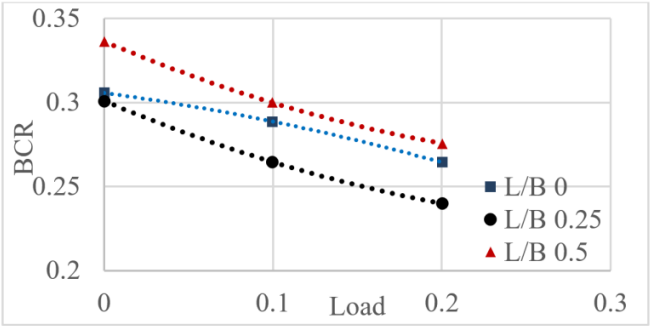

Fig. 11. BCR for soil II at H/B = 0.5.

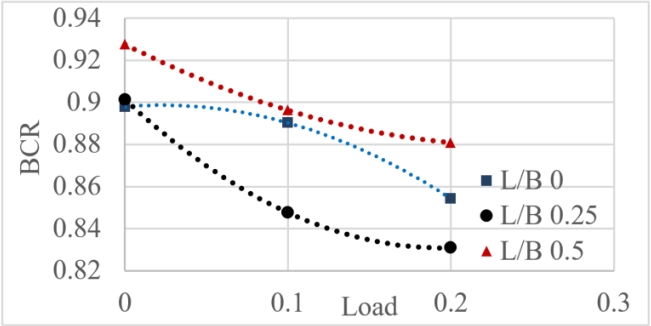

Fig. 12. BCR for soil I at H/B = 0.5.

Also, violin plots, as presented in Figures 14-17, were used for statistical evaluation, to assess how the engineering and geotechnical issues were affected by the soil's bearing capacity. This evaluation aims to characterize the data distribution patterns for all variables by presenting the primary statistical ranges and their corresponding sizes. It helps determine the variation within the dataset and the extent to which each parameter influences the outcomes. The reference soil registered/had the most extraordinary mean bearing capacity readings, accompanied by minimal fluctuation, suggesting good performance stability. The narrow distribution and lowest mean of soil III indicated widespread instability and low reliability in its geotechnical properties. A broader spread was observed in soils I and II, indicating efficiency variance due to the variation in the physical and mechanical properties of the samples, as shown in Figure 14.

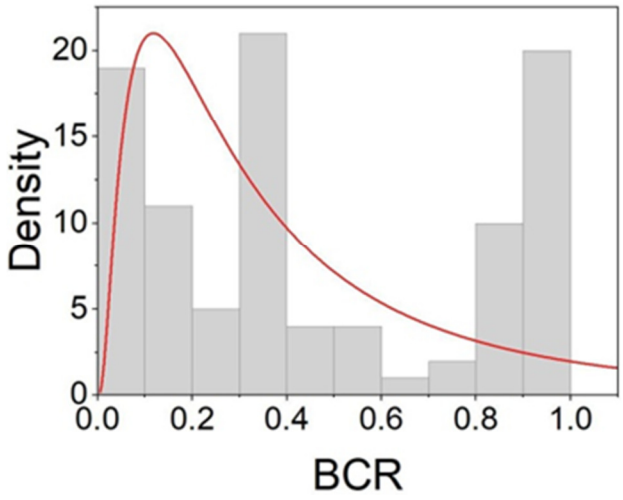

Fig. 13. Probability density distribution curve for BCR.

The concentrated loads performed better in terms of the load location, as they exhibited a uniform stress distribution and a comparatively small Interquartile Range (IQR), which suggests consistent results throughout the tests. On the other hand, the eccentric loads (Load 1 and Load 2) depicted in Figure 15, show an increase in variability and a drop in the average IQR, indicating that the stress was concentrated in particular regions of the soil. A dense range of outcomes was seen across every proportion as the influence of the height-to-width ratio (H/B) was examined, as portrayed in Figure 16. The mean bearing capacity gradually decreased as the ratio increased, illustrating how the vertical strains affecting the soil stability are influenced by the increasing relative height of the load.

Regarding the proportion (L/B), the concentrated loads (L/B = 0) performed most effectively since the stresses were well distributed and the variation was minimal. The average value was found to drop, and the variation was found to increase as the L/B ratio increased, as presented in Figure 17. This suggests that the greater distance impacts the unequal transfer of stresses. These statistical findings indicate that the current study enhances the understanding of the primary elements governing the soil performance, demonstrating the coupling between the engineering and geotechnical parameters.

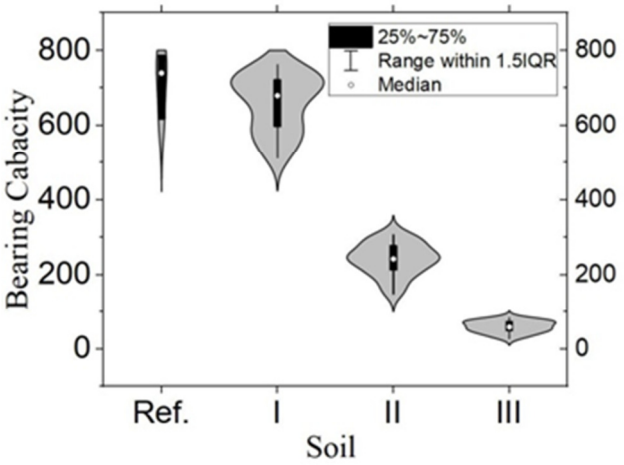

Fig. 14. Bearing capacity violin plot for soil types.

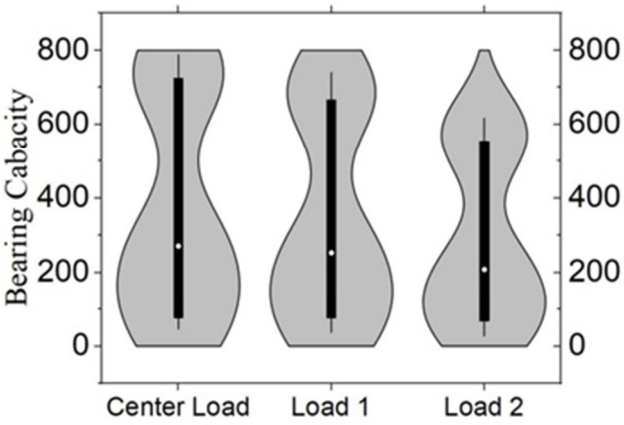

Fig. 15. Bearing capacity violin plot for load.

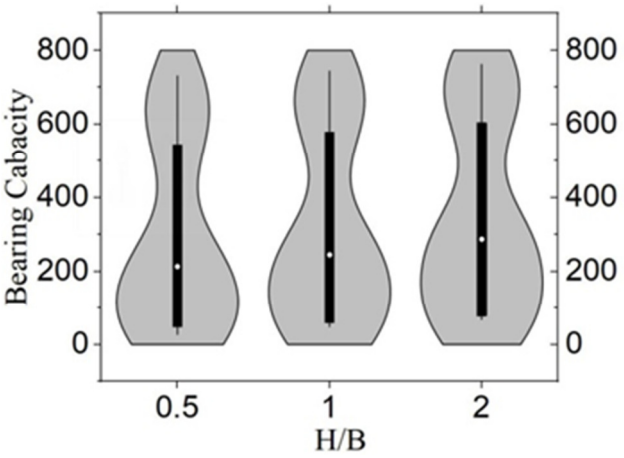

Fig. 16. Bearing capacity violin plot for H/B.

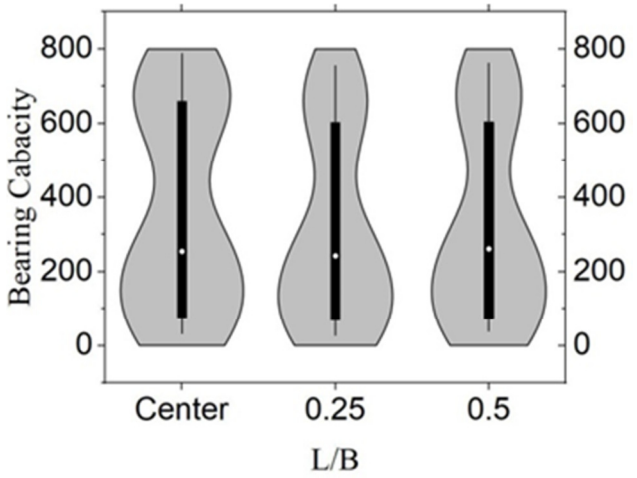

Fig. 17. Bearing capacity violin plot for L/B.

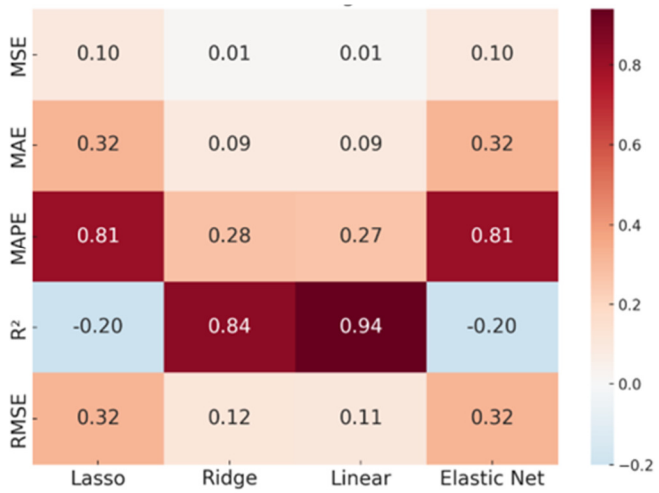

Fig. 18. Comparison of Linear, Ridge, and Elastic Net Regression models for BCR prediction.

VI. REGRESSION MODEL PERFORMANCE

The regression techniques enhance the analysis by supporting the development of a predictive model for estimating bearing capacity. In geotechnical engineering, the Linear Regression, Ridge Regression, and Elastic Net Regression models are used for modeling the relationship between the independent and dependent variables [18-19]. Table II summarizes the regression formulas along with the models' characteristics.

Figure 18 compares the performance of Linear Regression, Ridge Regression, and Elastic Net Regression models in predicting the data. As seen in Figure 18, Linear Regression is the most stable method, with the lowest mean square error and the highest coefficient of determination. Its ability to explain the variance in data is reflected in its stability. Ridge Regression, on the other hand, is stable and reduces variance without losing important features. However, Lasso and Elastic Net have poor performance, possibly due to the L1 regularisation, which may have removed important features and negatively affected the model's accuracy. Therefore, Linear Regression is used in the present study.

VII. LINEAR REGRESSION ANALYSIS

A linear regression analysis was conducted to study the effects of H/B, L/B, soil type, and e/B on the bearing capacity ratio. The results in Table III indicate that all variables have a statistically significant effect on BCR ($P < 0.05$), with varying signs of influence either positive or negative.

For H/B, the effect was adverse, with a coefficient of −0.0502, indicating that increasing H/B slightly reduces BCR. This behavior can be attributed to the increased vertical stresses on the soil caused by higher relative heights, which reduces stability. The $P = 0.045$ confirms the significance of this effect, though, it is relatively small. Similarly, L/B also showed an adverse effect, with a coefficient of −0.1664. This reflects the uneven stress distribution on the soil as the length-to-breadth ratio increases, reducing the soil's ability to bear loads. The $P = 0.047$ confirms the statistical significance of this effect.

In contrast, the soil type exhibited the most substantial positive effect, with a coefficient of +1.594, highlighting that improving the soil conditions significantly enhances BCR. Soils with good mechanical properties, such as cohesive or dense soils, can withstand higher stresses. The near-zero P value supports this conclusion.

For e/B, the effect was adverse, with a coefficient of −0.5613. An increased eccentricity-to-breadth ratio reduces BCR, likely due to asymmetric stress distributions caused by eccentricity, which leads to reduced stability. The $P = 0.008$ confirms the significance of this variable.

Based on these findings, priority should be given to improving the soil quality and minimizing the effects of eccentricity by ensuring a balanced load distribution. Optimizing the geometric design ratios (H/B and L/B) can also help mitigate the adverse impacts on BCR.

This study underscores the importance of considering both the sign and magnitude of the effects of influencing factors on the soil performance. Further research is proposed to explore factors, such as relative density and moisture content, for a greater understanding of the bearing capacity.

The equation for the BCR of the soil is expressed by (Table IV):

$$BCR = -0.46 + 0.05\left(\frac{H}{B}\right) + 0.035\left(\frac{L}{B}\right) + 2.1(\omega\%) - 0.044\left(\frac{e}{B}\right) \quad (1)$$

While the proposed model offers valuable insights into the impact of the gypsum content, dissolution percentage, cavity location, and loading conditions on the foundation stability, its validity is limited to the specific soil types and controlled conditions employed in this study. Therefore, the results should not be generalized without further validation. Future work should test the model under a wider range of field conditions and soil types to ensure broader applicability.

TABLE II. REGRESSION TECHNIQUES

Aspect	Linear Regression	Ridge Regression	Elastic Net Regression
Description	Establishes a linear relationship between dependent and independent variables.	A modified linear regression that includes an L2 penalty term to reduce overfitting.	Combines L1 (Lasso) and L2 (Ridge) penalties to balance regularization and feature selection.
Regularization type	None (pure Ordinary Least Squares - OLS).	L2 Regularization (Ridge Penalty).	Combines L1 (Lasso) and L2 (Ridge) penalties for feature selection and stability.
Impact on coefficients	No shrinkage; all features contribute equally.	Shrinks coefficients toward zero but never precisely zero.	Some coefficients shrink to zero (L1), while others remain small (L2).
Overfitting handling	Prone to overfitting with high-dimensional data.	Reduces overfitting by penalizing significant coefficients.	Balances feature selection and stability, valid for collinear data.
Best use cases	Small datasets, low multicollinearity.	High-dimensional data prevent overfitting but retain all features.	When feature selection and regularization are needed.
Applications	Used for initial BCR estimations and identifying the key influencing factors in soil behavior.	Applied when strong correlations exist among the geotechnical parameters.	Ideal for high-dimensional datasets with complex relationships.
Mathematical formula	Linear Regression: $Y = \beta_0 + \beta_1 X_1 + \beta_2 X_2 + \cdots + \beta_n X_n + \epsilon$		
	Ridge Regression: $Y = \beta_0 + \sum_{i=1}^{n} \beta_i X_i + \lambda \sum_{i+1}^{n} \beta_i^2$		
	Elastic Net Regression: $Y = \beta_0 + \sum_{i=1}^{n} \beta_i X_i + \sum_{i+1}^{n} \beta_i X_i \, 1 \sum_{i+1}^{n} \| \beta i \| + \lambda 2 \sum_{i=1}^{n} \beta_i^2$		

TABLE III. OUTPUT OF LINEAR REGRESSION MODEL

	Coefficients	Standard error	t-Stat	P-value	Lower 95%	Upper 95%	Lower 95.0%	Upper 95.0%
H/B	-0.1	0.0	-2.0	0.0	-0.1	0.0	-0.1	0.0
L/B	-0.2	0.1	-2.0	0.0	-0.3	0.0	-0.3	0.0
Soil type	1.6	0.1	18.0	0.0	1.4	1.8	1.4	1.8
e/B	-0.6	0.2	-2.7	0.0	-1.0	-0.2	-1.0	-0.2

TABLE IV. REGRESSION STATISTICS

Multiple R	0.964
R square	0.930
Adjusted R square	0.914
Standard error	0.152

VIII. CONCLUSIONS

Despite considerable research on foundation performance in soluble soils, the effects of cavity geometry—specifically, cavity depth and horizontal position relative to foundation centers—and load eccentricity on the bearing capacity are not fully understood. This study addresses these gaps through Finite Element Modeling (FEM) of gypsum soils with varying degrees of dissolution.

The results indicate that increasing the cavity depth relative to its horizontal offset reduces the direct impact of cavitation on the stress distribution, decreasing the load-induced stress concentrations and improving the bearing capacity, especially in soils with low dissolution levels. Soils with higher dissolution rates exhibited limited improvement due to the structural weakening caused by extensive cavitation. Shifting the load positions horizontally away from the cavities promotes a more uniform stress distribution and higher bearing capacity, while the loads applied directly above the cavities result in a localized stress concentration and reduced performance.

Soils without dissolution consistently demonstrated the highest bearing capacity, whereas increased dissolution levels corresponded with significant reductions in the load-bearing capacity. The statistical analysis identified the dissolution rate as the dominant factor influencing the variations in bearing capacity. A predictive regression model was developed to quantify the combined effects of the cavity geometry and load position on the bearing capacity.

This research enhances the understanding of the mechanical and geometrical influence on foundation performance in gypsum soils, providing practical insights and predictive tools to optimize the foundation design and mitigate failure risks in soluble soil environments.

REFERENCES

[1] P. N. Quang, O. Satoru, I. Koichi, and F. Yutaka, "Bearing Capacity of Footing Resting on Sand for Eccentric Vertical Load," in *Geotechnics for Sustainable Infrastructure Development*, vol. 62, P. Duc Long and N. T. Dung, Eds. Singapore: Springer Singapore, 2020, pp. 1135–1142.

[2] G. Wu, M. Zhao, R. Zhang, and G. Liang, "Ultimate bearing capacity of eccentrically loaded strip footings above voids in rock masses," *Computers and Geotechnics*, vol. 128, Dec. 2020, Art. no. 103819, https://doi.org/10.1016/j.compgeo.2020.103819.

[3] L. Zhao, S. Huang, Z. Zeng, R. Zhang, G. Tang, and S. Zuo, "Study on the ultimate bearing capacity of a strip footing influenced by an irregular underlying cavity in karst areas," *Soils and Foundations*, vol. 61, no. 2, pp. 259–270, Apr. 2021, https://doi.org/10.1016/j.sandf.2020.09.011.

[4] A. Nezari, R. Boufarh, and T. Mansouri, "Numerical Investigation of Bearing Capacity of Centrally and Eccentrically Loaded Surface Footing on Sand-Clay with Void Using Plaxis 2D," *The Journal of Engineering and Exact Sciences*, vol. 10, no. 3, Apr. 2024, Art. no. 17506, https://doi.org/10.18540/jcecvl10iss3pp17506.

[5] E. K. Lukueta and K. Isobe, "Bearing Capacity of a Shallow Foundation above the Soil with a Cavity Based on Rigid Plastic Finite Element Method," *Applied Sciences*, vol. 14, no. 5, Feb. 2024, Art. no. 1975, https://doi.org/10.3390/app14051975.

[6] P. A. Jeyaseelan and M. Madhavan, "Application of FEM and Artificial Intelligence Techniques (LRM, RFM & ANN) in Predicting the Ultimate Bearing Capacity of Reinforced Soil Foundation," *Buildings*, vol. 14, no. 8, Jul. 2024, Art. no. 2273, https://doi.org/10.3390/buildings14082273.

[7] A. Benbouza, T. Mansouri, and K. Abbeche, "Behavior of Strip Footing/s above Void in Sandy Soil," *Engineering, Technology & Applied Science Research*, vol. 13, no. 1, pp. 10039–10044, Feb. 2023, https://doi.org/10.48084/etasr.5494.

[8] M. Kazemzadeh, P. Pezeshkian, A. Zad, and M. Yazdi, "Behavior of a Foundation Built on Geogrid-Reinforced Sand in the Presence of Twin Subsurface Voids," *International Journal of Geosynthetics and Ground Engineering*, vol. 10, no. 5, 2024, Art. no. 82.

[9] S. Alzabeebee, B. H. Ismael, S. Keawsawasvong, and J. T. Chavda, "Finite element and evolutionary polynomial regression analyses of the effect of a cavity on the bearing capacity factor Nc of strip footing," *Modeling Earth Systems and Environment*, vol. 10, no. 3, pp. 3815–3826, Jun. 2024, https://doi.org/10.1007/s40808-024-01985-6.

[10] T. Mansouri, R. Boufarh, and D. Saadi, "Effects of underground circular void on strip footing laid on the edge of a cohesionless slope under eccentric loads," *Soils and Rocks*, vol. 44, no. 1, pp. 1–10, Mar. 2021, https://doi.org/10.28927/SR.2021.055920.

[11] A. M. Rajabi, M. Saadati, M. Mahmoudi, and E. Fijani, "Effect of the circular cavity on the undrained bearing capacity of shallow strip footing," *Arabian Journal of Geosciences*, vol. 15, no. 14, Jul. 2022, Art. no. 1265, https://doi.org/10.1007/s12517-022-10503-w.

[12] S. Keawsawasvong, V. Q. Lai, C. Thongchom, and C. N. Van, "Undrained Bearing Capacity of Circular Footing Above Spherical Cavity," in *Computational Intelligence Methods for Green Technology and Sustainable Development*, vol. 567, Y.-P. Huang, W.-J. Wang, H. A. Quoc, H.-G. Le, and H.-N. Quach, Eds. Cham, Switzerland: Springer International Publishing, 2023, pp. 190–200.

[13] M. M. Jasim, R. M. Al-Khaddar, and A. Al-Rumaithi, "Prediction of bearing capacity, angle of internal friction, cohesion, and plasticity index using ANN (Case Study of Baghdad, Iraq)," *International Journal of Civil Engineering and Technology*, vol. 10, no. 1, pp. 2670–2679, Jan. 2019.

[14] B. Azeddine and M. Abdelghani, "The cavity's effect on the bearing capacity of a shallow footing in reinforced slope sand," *Soils and Rocks*, vol. 46, no. 1, Jan. 2023, Art. no. e2023003622, https://doi.org/10.28927/SR.2023.003622.

[15] A. Al-Obaidi and R. S. Najim, "Estimation of Bearing Capacity Dropping Due to Cavities from Gypseous Soils Melting," *Key Engineering Materials*, vol. 857, pp. 409–416, Aug. 2020, https://doi.org/10.4028/www.scientific.net/KEM.857.409.

[16] A. A. J. Jamel and M. I. Ali, "Stability and seepage of earth dams with toe filter (Calibrated with Artificial Neural Network)," *Journal of Engineering Science and Technology*, vol. 16, no. 5, pp. 3712–3725, Oct. 2021.

[17] A. M. Ahmed, S. I. Ali, M. I. Ali, and A. A. J. Jamel, "Analyzing Self-Compacted Mortar Improved by Carbon Fiber Using Artificial Neural Networks," *Annales de Chimie - Science des Matériaux*, vol. 47, no. 6, pp. 363–369, Dec. 2023, https://doi.org/10.18280/acsm.470602.

[18] A. K. M. E. Saleh, B. M. G. Kibria, B. M. G. Kibria, and M. Arashi, *Theory of ridge regression estimation with applications*. Hoboken, NJ: Wiley Blackwell, 2019.

[19] A. A. J. Jamel, "The Effect of Rainfall Intensity on Slope Stability: An Analytical Study using Numerical Modeling," *Engineering, Technology & Applied Science Research*, vol. 15, no. 2, pp. 21203–21207, Apr. 2025, https://doi.org/10.48084/etasr.10257.